Fast removal of cationic dyes using pH-sensitive Fe_3O_4/poly(methacrylic acid) nanocomposite particles

N. Saadatjoo[a], M. Hayasi[a], M. Karimi[b],*

[a]*Faculty of Chemistry, Department of Applied Chemistry, Semnan University, Semnan, Iran, Tel. +98 23 3338 3194; emails: nsaadatjoo@semnan.ac.ir (N.Saadatjoo), mozhgan_hayasi@yahoo.com (M. Hayasi)*
[b]*Department of Textile Engineering, Amirkabir University of Technology, Hafez Avenue, 15914 Tehran, Iran, Tel. +98 21 6454 2658; Fax: +98 21 66400245; email: mkarimi@aut.ac.ir*

ABSTRACT

In this work, the pH-sensitive magnetic Fe_3O_4/polymethacrylic acid nanocomposite particles were synthesized by a new one-step method and used as adsorbents for the removal of two cationic dyes from aqueous solution. The resulting product was characterized using Fourier transform infrared spectra, transmission electron microscopy (TEM), thermogravimetric analysis, and vibrating sample magnetometer. Particles size distribution of product and its pH responsivity was investigated by dynamic light scattering. Adsorption performance of the magnetic adsorbent was tested with removal of methylene blue and maxilon red GRL from aqueous solution. The effects of solution pH value, adsorption time and initial dye concentration were investigated. The adsorption behavior fits well with the Langmuir rather than the Freundlich model. The results reveal that the adsorbent has ability to remove dyes rapidly within a few minutes due to the absence of the internal diffusion resistance. Moreover, the synthesized adsorbent has good reusability.

Keywords: Fe_3O_4 nanoparticle; Surface modification; Polymethacrylic acid; Cationic dyes; pH sensitive; Adsorption

1. Introduction

Water contamination is one of the most unfavorable environmental problems in the world. Among contaminants, dyes are harmful to our environment due to their toxicity [1–3]. Pollution of water by dyes even at low concentration is undesirable for human consumption [4]. A large variety of dyes are produced on a daily basis in textile, leather, paper, and food industries [5]. Thus, the removal of dyes from effluents is of most importance. Among the various techniques for dye removal from wastewater, such as adsorption, electrochemical treatment, coagulation, precipitation, and solvent extraction [6–8], adsorption is an effective method particularly for its simplicity, low cost, ease of operation, and ease of availability [9,10]. Many works have been done for the development of new adsorbents with a large surface area, enhanced adsorption rate, selectivity for adsorbates, and easy separation properties [11]. Various adsorbents have been used to remove dyes from wastewater such as activated carbon [12], kaolin [13], montmorillonite clay [14], halloysite nanotube [15], polymeric materials [16], etc. Among these adsorbents,

*Corresponding author.

nanoparticles have gained considerable attention for the removal of dyes because of their high surface area to volume ratio and ease of modifying their surface but the difficulty for separating them from the aqueous phase limits their application potential in effluent purification. Thus, it is necessary to use an adsorbent that does not generate secondary waste and easily be separated.

Compared to the traditional adsorbents, magnetic nanomaterials not only have high efficient specific surface area and fast kinetics but also have high separation efficiency and reusability [17,18]. However, uncoated magnetite nanoparticles are fully sensitive to air oxidation and are easily aggregated in aqueous systems. To prevent the agglomeration of nanoparticles, various stabilizers have been applied for stabilizing nanoparticles, such as surfactant [19] and polymers [20,21]. Polymers coating on the surface of magnetic nanoparticles prevent particle agglomeration and improve the dispersion stability of the nanostructures in suspension medium [22,23]. In addition, these polymeric coatings can also provide functional groups for conjugation with various compounds such as dyes.

In recent years, many studies have been done for the modification of the magnetic nanoparticles to provide a better surface specificity for the removal of different dyes from aqueous solutions. For instance, Zhu et al. prepared Chitosan/kaolin/nanosized γ-Fe$_2$O$_3$ composites by a microemulsion process and used these materials for the adsorption of methyl orange [24]. Adsorption behavior of Fe$_3$O$_4$ magnetic nanoparticles modified with 3-glycidoxypropyltrimethoxysilane (GPTMS) and glycine (Gly) for the removal of anionic and cationic dyes has been reported [25]. The removal of rhodamine 6G by hexadecyl functionalized magnetic silica nanoparticles has been done [26]. Li et al. synthesized a magnetic nanomaterial modified with aminoguanidine for the adsorption of acid dyes [27]. Zargar et al. prepared magnetic nanoparticles coated with cetyltrimethyl ammonium bromide (CTAB) as an adsorbent for the removal of amaranth from water solution [28]. Zhang and Kong synthesized magnetic Fe$_3$O$_4$/C core–shell nanoparticles by a simple method and used as adsorbents for the removal of organic dyes from aqueous solution and adsorption behavior of these adsorbents were tested with removal of methylene blue (MB) and cresol red from aqueous solution [29]. Furthermore, adsorbents based on biopolymer–magnetic nanoparticles have been reported for the removal of dyes [30–33].

In this study, a pH-sensitive magnetic adsorbent based on Fe$_3$O$_4$/poly(methacrylic acid)is synthesized and used for the removal of cationic dyes such as MB and maxilon red GRL (MR GRL) from aqueous

solution. The physical and chemical characterization of the Fe$_3$O$_4$/polymethacrylic acid (PMAA) nanocomposites particles is investigated. The effects of pH, initial dye concentration and contact time on the adsorption behavior of the magnetic adsorbents are also studied. Moreover, the recycling and reuse of the used adsorbents is also performed for its great importance in practical applications.

2. Experimental

2.1. Materials

Iron oxide nanoparticles (Fe$_3$O$_4$, purity: >99.5%, 15–20 nm) were purchased from US Research Nanomaterials, Inc. Methacrylic acid monomer, N,N-methylene-bis-acrylamide (MBA) as crosslinker, ammonium persulfate (APS) as initiator and sodium dodecyl sulfate (SDS) as surfactant were acquired from Sigma–Aldrich Co., Ltd. Methanol, sodium hydroxide (NaOH), hydrochloric acid (HCl) and acetic acid were supplied from Merck Chemical Co. MB and MR GRL were obtained from Ciba Co. All these chemicals were used without further purification. The chemical structures of MB and MR GRL are illustrated in Fig. 1.

2.2. Synthesis of Fe$_3$O$_4$/PMAA nanocomposites particles

In a three-neck round-bottom flask, Fe$_3$O$_4$ nanoparticles (0.264 g) and MAA monomer (0.13 ml) were mixed in 100 ml of deionized water (DI), and ultrasonicated for 25 min in an ice bath. Then, MAA (3 ml), MBA (0.0564 g), and SDS (0.62 g) were mixed in 80 ml of DI water and added to a suspension containing the Fe$_3$O$_4$ and MAA. This mixture was stirred at 300 rpm for 40 min under a nitrogen atmosphere and heated to 75°C. 0.17 g APS as initiator was dissolved in 25 ml of DI water and then added to the above mixture during the reaction. Reaction was performed for 5 h under a
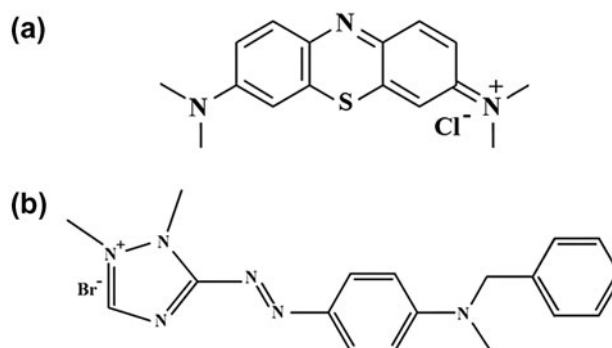

Fig. 1. The structures of MB (a) and MR GRL (b).

nitrogen atmosphere. The synthesized particles were washed with DI water and dried in vacuum oven at 50°C overnight. Fig. 2 shows the procedure for the synthesis of Fe_3O_4/PMAA nanocomposites particles.

2.3. Characterization

Fourier transform infrared (FT-IR) spectra were determined on a Nicolet Nexus 670 FT-IR spectrometer within the range of 500–4,000 cm^{-1} with the resolution of 4 cm^{-1} and using of KBr pellets. Transmission electron microscopy (TEM) images were taken on a Philips CM30 TEM operated at 200 kV; samples were dispersed in distilled water at an appropriate concentration, cast onto a carbon-coated copper grids and then dried under vacuum. Hydrodynamic diameters (D_h) of the particles were measured by dynamic light scattering (DLS) with a NanoBrook 90Plus particle size analyzer at a fixed scattering angle of 90° and the concentration of each sample was 5 mg L^{-1} DI. The magnetic property of the samples was investigated using a vibrating sample magnetometer (VSM) with an applied field from +10 kOe to −10 kOe at room temperature (Magneto Kavir Co). Thermogravimetric

analysis (TGA) was carried out with a TGA Q50 V6.3 Build 189 thermogravimetric analyzer at heating rate of 20°C/min in the temperature range of 25–600°C under argon atmosphere. Cationic dye concentration in solution was determined using a JENWAY 6105 UV–visible spectrophotometer at λ_{max} = 530 nm for MR, λ_{max} = 664 nm for MB. The ultrasonication device Model UP200S (200 W, 24 kHz) from Hielscher GmbH was used for rising the dispersion of nanoparticles inside of the samples.

2.4. Adsorption and desorption experiments

In general, 5 mg of adsorbent was added to 5 ml of cationic dyes solution of desired concentration and shaken over a period of time on a shaker at 170 rpm. The samples were removed from the solution by magnetic separation. The effects of contact time (5–60 min), initial concentrations (10–350 mg L^{-1}) were examined throughout the experiments. The effect of pH on adsorption of dye was also studied over a pH range of 2.0–10.0. The pH was adjusted by adding aqueous solutions of 1 mol L^{-1} HCl or 1 mol L^{-1} NaOH using a pH meter. At higher pH, it was very
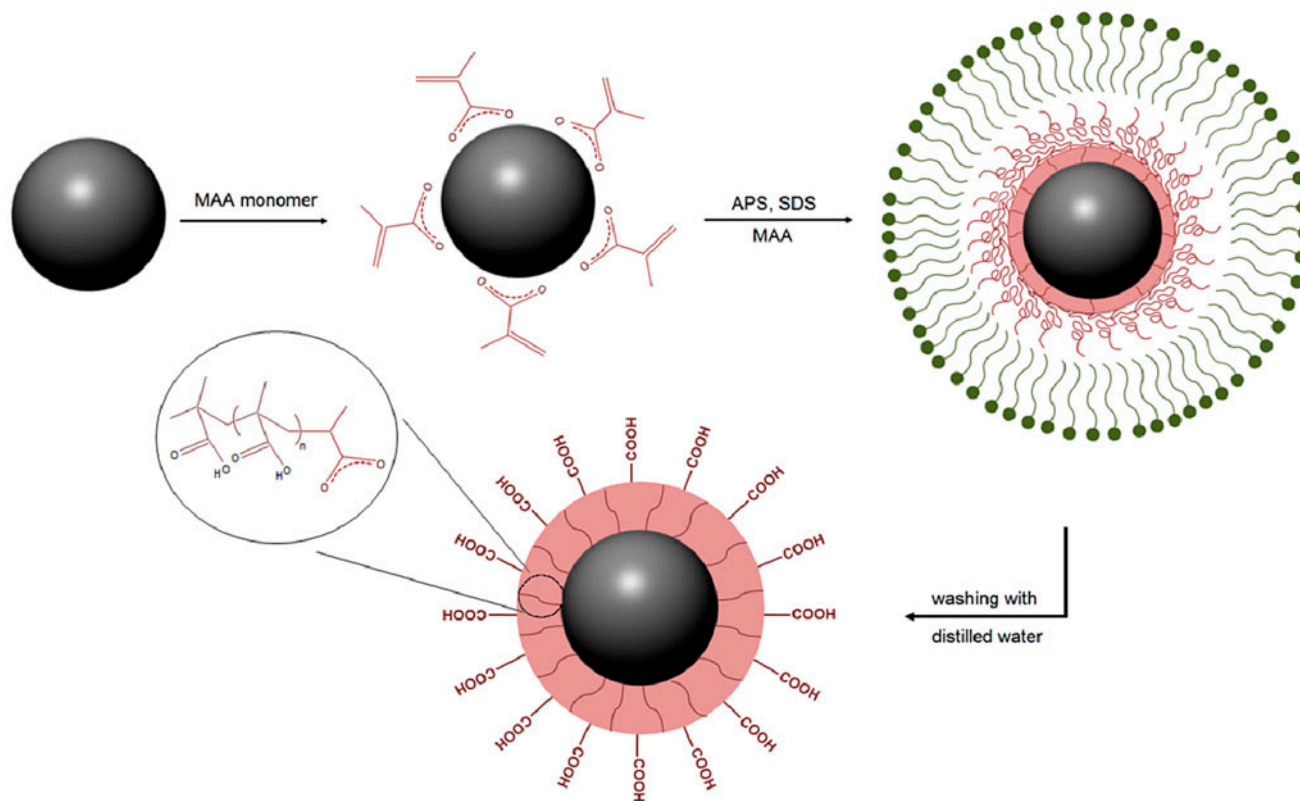

Fig. 2. Schematic diagram for synthesis of Fe_3O_4/PMAA nanocomposite particles.

difficult to investigate the adsorption behavior accurately, because many cationic dyes are unstable under strong alkaline conditions [34]. The adsorption capacity in experiments, q (mg g^{-1}), was calculated according to the following equation:

$$q = \frac{(C_0 - C_e)V}{m} \qquad (1)$$

where q (mg g^{-1}) is the amount adsorbed per gram of adsorbent, C_0 and C_e are the initial and equilibrium concentrations of dye in the solution (mg L^{-1}), respectively, m is the mass of the adsorbent used (g), and V (L) is the initial volume of the dye solution.

For desorption, the magnetic material containing dye was sonicated with 5 ml of methanol solution containing 10% acetic acid for 10 min. The adsorbent was collected by a magnet, then washed with DI water and reused for adsorption again. This process was repeated four times.

3. Results and discussion

3.1. Characterization of Fe₃O₄/PMAA nanocomposite particles

Structure of the synthesized nanocomposite particles was characterized by FTIR spectroscopy. Fig. 3 shows the FTIR spectra of the Fe₃O₄ nanoparticles and Fe₃O₄/PMAA nanocomposite particles. According to the Fig. 3(b), the strong peak at 575 cm^{-1} corresponds to the characteristic band of Fe–O vibration. The peaks

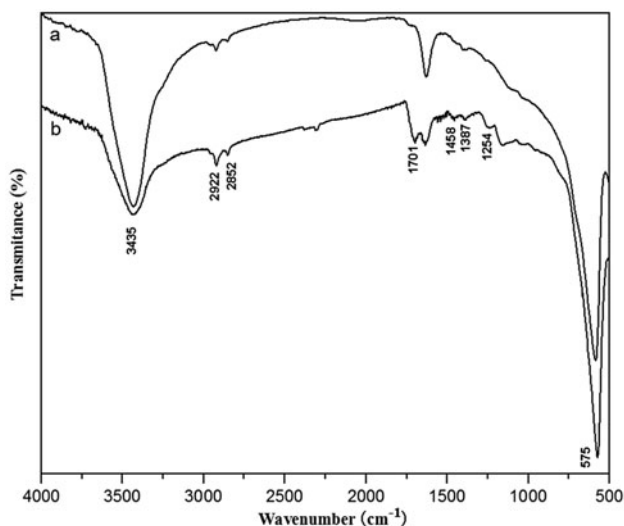Fig. 4. Thermogravimetric curves of Fe₃O₄ nanoparticles (a) and Fe₃O₄/PMAA (b).

around 1,701 and 1,254 cm^{-1} are related to the C=O and C–O stretching vibration of carboxyl groups, respectively, the broad band around 3,435 cm^{-1} can be assigned to the O–H stretching vibrations of carboxyl groups and adsorbed water. The peaks at around 2,922 and 2,852 cm^{-1} are ascribed to the CH₂ stretching vibrations; the C–O–H bending vibration is in the region 1,458–1,387 cm^{-1}. These results indicate that surface of Fe₃O₄ nanoparticles successfully coated with PMAA.
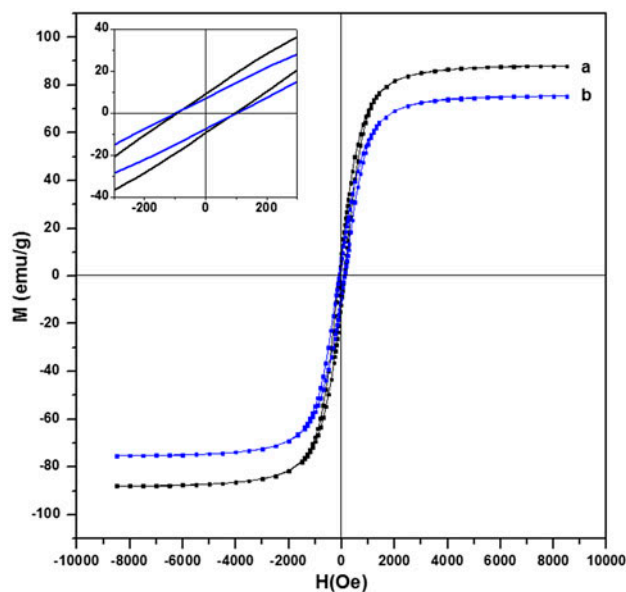

Fig. 3. FT-IR spectra of bare Fe₃O₄ (a) and Fe₃O₄/PMAA (b).

Fig. 5. Magnetization curves at room temperature of bare Fe₃O₄ (a) and Fe₃O₄/PMAA (b).

Table 1
Magnetic properties of magnetic samples

Sample	M_s (μ g^{-1})	M_r (μ g^{-1})	M_r/M_s	H_c (Oe)
Fe$_3$O$_4$	87	9	0.103	94
Fe$_3$O$_4$/PMAA	75	7	0.093	99

The result of TGA for PMAA-coated magnetic nanoparticles is shown in Fig. 4. We can determine the amount of PMAA coated on the surface of Fe$_3$O$_4$ nanoparticles using this analysis. The first mass losses within the range of 25–250°C can be attributed to water desorption. The second mass loss between 250 and 500°C is attributed to the thermal decomposition
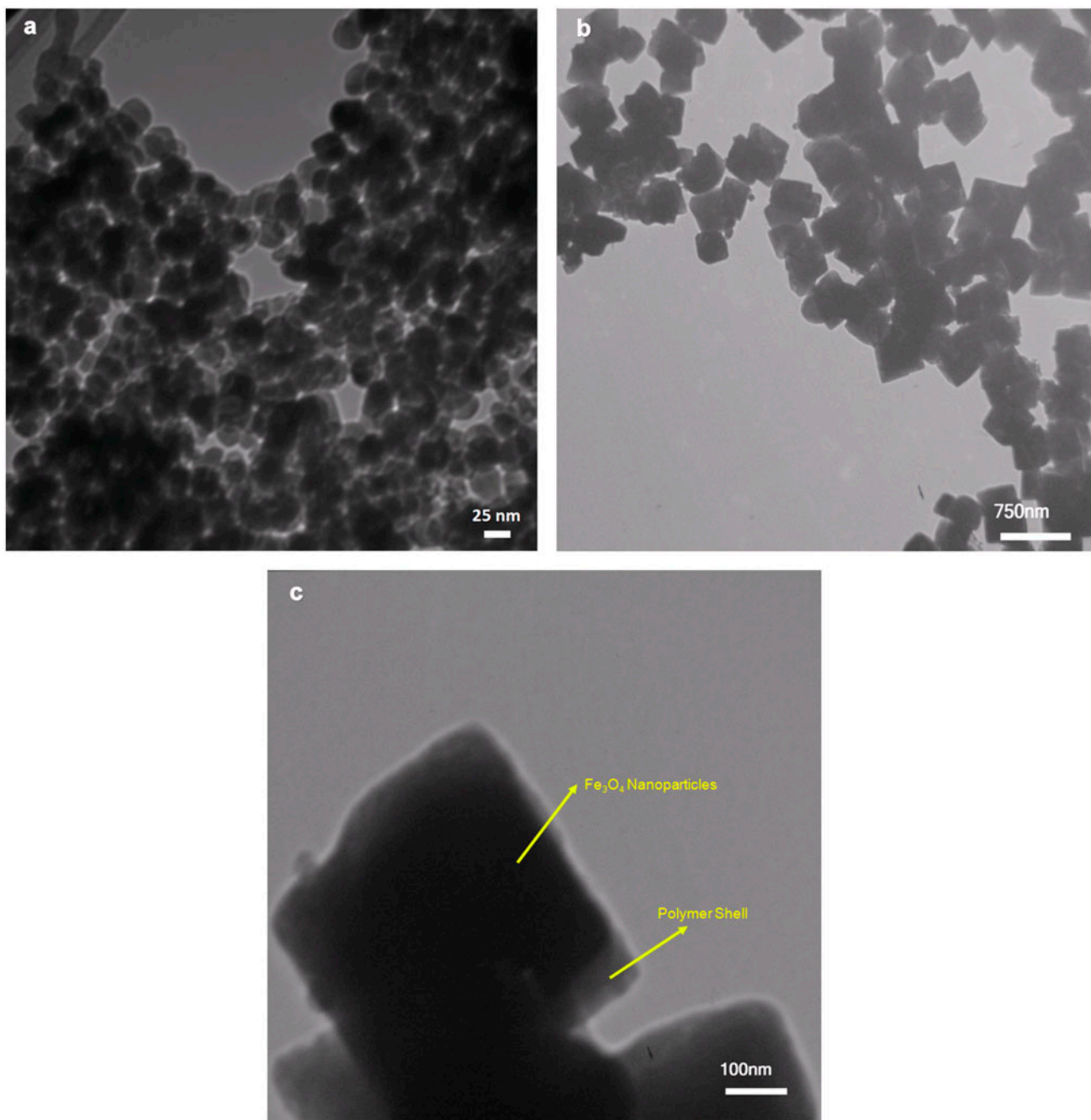

Fig. 6. TEM image of Fe$_3$O$_4$ nanoparticles (a) and Fe$_3$O$_4$/PMAA nanocomposite particles (b and c).
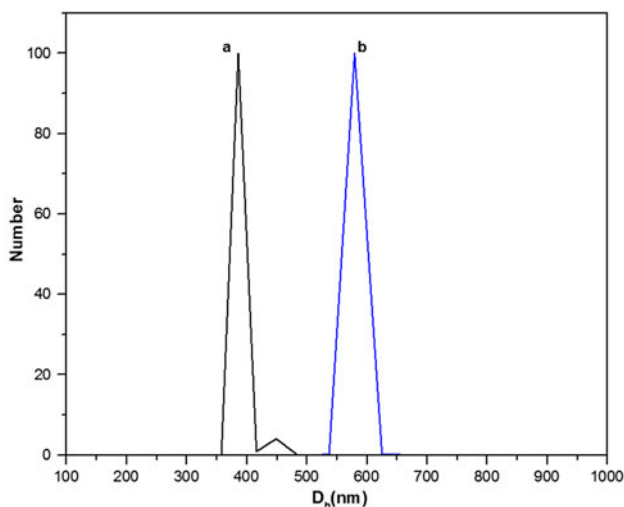
Fig. 7. Hydrodynamic diameter and size distribution of Fe$_3$O$_4$/PMAA nanocomposite particles at pH 2.5 (a) and pH 9.5 (b) as determined by DLS.

of PMAA coated on magnetic nanoparticles (Fig. 4(b)). TGA curve shows that the percentage of coated polymer is about 5%, indicating the particles contain high inorganic magnetite. Therefore, nanocomposite particles possess high magnetic sensitivity under an external magnetic field and can be easily separated from the water phase.

VSM was employed to compare the magnetic property of Fe$_3$O$_4$ nanoparticles and synthesized Fe$_3$O$_4$/PMAA nanocomposites particles. As shown in Fig. 5, the saturation magnetization value of Fe$_3$O$_4$ nanoparticles was 87 μ g^{-1} at room temperature. After coating of Fe$_3$O$_4$ nanoparticles by PMAA, the saturation magnetizations reduced to 75 μ g^{-1}. The decrease in the saturation magnetization is related to the non-

magnetic contribution of the polymer shell surrounding the Fe$_3$O$_4$ nanoparticles. The polymer coating alters surface magnetic anisotropy and leads to an increase of the surface spins disorientation [35]. The saturation magnetization (M_s), the remanent magnetization (M_r) per gram of samples, the coercivities (H_c), and their remanences (calculated from remanent magnetization divided by saturation magnetization) were listed in Table 1. The results showed almost low coercivity and remanence, exhibiting characteristics of soft magnetic materials. Also Fe$_3$O$_4$/PMAA has high saturation magnetization (75 μ g^{-1}) that reflects the ability of product to respond very fast to an external magnetic field.

Fig. 6 shows the TEM image of the Fe$_3$O$_4$ nanoparticles and synthesized Fe$_3$O$_4$/PMAA nanocomposite particles. As shown in Fig. 6(a) Fe$_3$O$_4$ nanoparticles have average diameter about 20 nm. As seen in Fig. 6(c), the black particles are Fe$_3$O$_4$, and polymer shell is gray. It is clear to see that polymer shell has surrounded magnetite nanoparticles and these particles have been successfully encapsulated inside polymer shell. Also, the resulting nanocomposite particles have good dispersibility with average size of about 390 nm. Furthermore, Fe$_3$O$_4$/PMAA nanocomposite particles have cubic structures. We expected that the nanocomposite particles have spherical structures but they showed cubic structures. This may be related to the self-assembly of Fe$_3$O$_4$ nanoparticles like cubic shape and growth of polymer chains around these structures. A similar result has been observed for oligoamino-ester graft-from magnetite nanoparticles previously [36].

The pH sensitivity characteristics of the Fe$_3$O$_4$/PMAA particles were determined using DLS in aqueous solutions by investigating the change of particles size at two pH values. The hydrodynamic diameter (D_h) and size distribution of the Fe$_3$O$_4$/PMAA
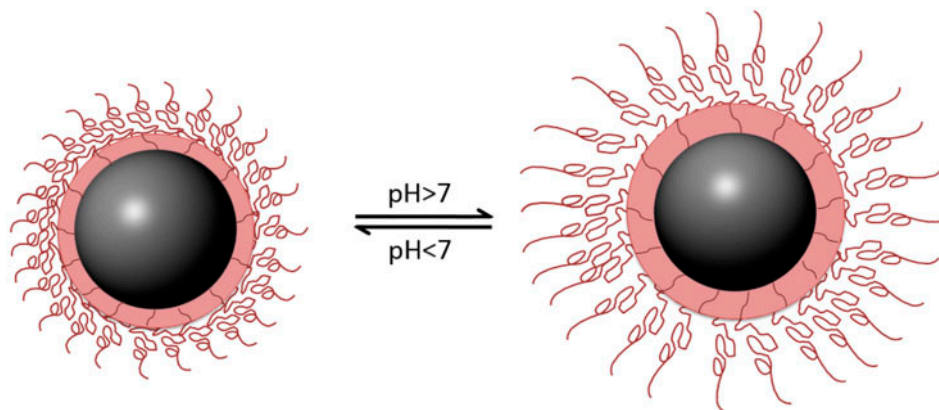

Fig. 8. Schematic illustration of pH sensitive Fe$_3$O$_4$/PMAA nanocomposite particles.
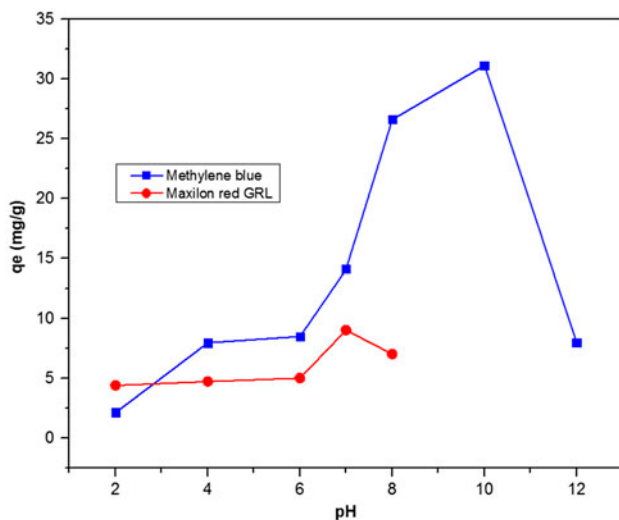
Fig. 9. Effect of pH on adsorption of MB and MR GRL by Fe$_3$O$_4$/PMAA. C_{dye}: 50 mg L^{-1}, Temperature: 25℃.

Fig. 10. Effect of time on adsorption of MB and MR GRL by Fe$_3$O$_4$/PMAA, pH 7.0 for MR GRL, pH 10 for MB, Temperature: 25℃ (a) and intra particle model for adsorption of MB and MR GRL on to Fe$_3$O$_4$/PMAA (b).

nanocomposite particles at pH 2.5 and pH 9.5 are shown in Fig. 7. From the curves of particles size distribution for Fe$_3$O$_4$/PMAA nanocomposite particles, it becomes clear that a single peak was appeared and the average D_h of particles at pH 2.5 was 392 nm, much lower than 579 nm at pH 9.5. Increasing of particles size at high pH is related to ionization of most carboxylic groups along the PMAA chains and swelling of PMAA shell due to electrostatic repulsions. In the acidic medium, the protonation of most carboxylic groups is occurred, and the shell of PMAA is collapsed (Fig. 8). Polydispersity index (PDI) values based on DLS of these samples were less than 0.01, confirming high monodispersity of samples. The average D_h of particles at pH 2.5 was consistent with the average diameter estimated from the TEM image.

3.2. Adsorption studies

3.2.1. Effect of pH

The effect of the initial pH on the adsorption capacity of dyes by Fe$_3$O$_4$/PMAA nanocomposite particles was studied over the pH range from 2.0 to 10.0; the results are shown in Fig. 9. As can be seen from Fig. 9, the adsorption capacity increases with increasing the pH of dye solution. Electrostatic interaction could play an important role on dye adsorption onto Fe$_3$O$_4$/PMAA particles at various pH values. With increasing pH, most of the carboxylic groups are ionized and changed to carboxylate anions thus they can efficiently interact with the amino groups of the dyes by positive charge. Moreover, the volume expansion
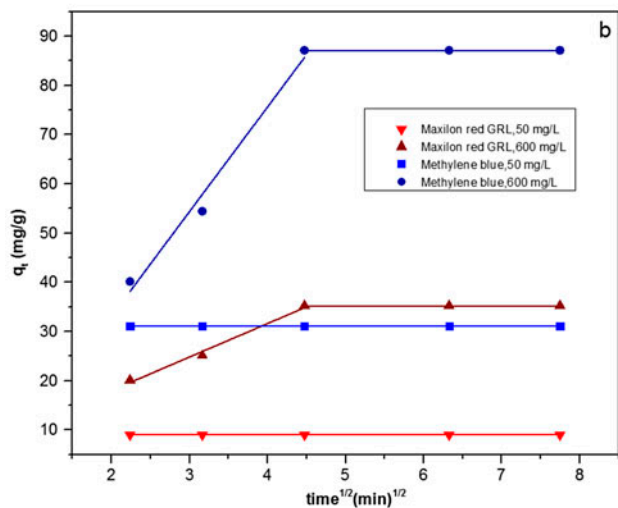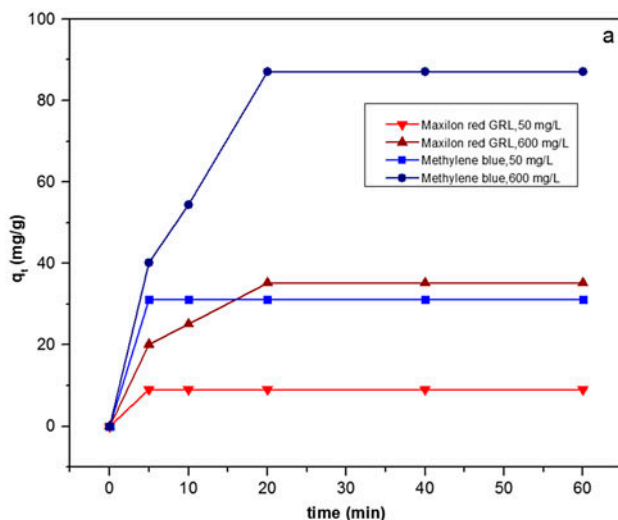
in the polymer network due to the electrostatic repulsion among the polymer chains at basic pH can enhance the adsorption of cationic dyes. In addition, the weaker dyes adsorption under lower solution pH can be attributed to protonation of carboxylic groups of the methacrylic acid. As shown in Fig. 9, removal of MB dye at pH > 10 and MR GRL dye at pH > 7, decreased with increasing the pH value. This might be attributed to the structural changes of dyes molecules at this two pH values [37,38].

3.2.2. Effect of contact time

Fig. 10 shows the adsorption rate of MB and MR GRL on Fe$_3$O$_4$/PMAA particles. The adsorption
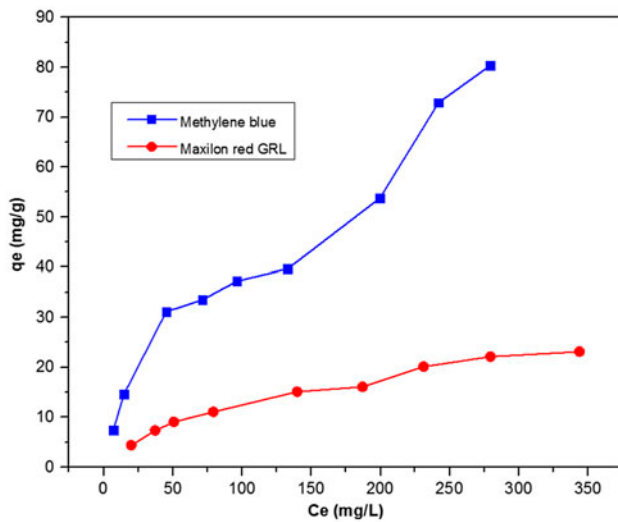
Fig. 11. Equilibrium isotherms of cationic dyes by Fe_3O_4/PMAA. pH 7.0 for MR GRL, pH 10 for MB, Cationic dyes 10–350 mg L^{-1}, Temperature: 25°C, Time: 5 min.

capacity of dyes at the contact time from 5 to 60 min had no significant differences at low concentration of dyes (50 mg L^{-1}) and the adsorption equilibrium was reached within 5 min. But at high concentration of dyes (600 mg L^{-1}), the adsorption reached equilibrium within 20 min. It might be attributed to occupation of active sites by the dye molecules at higher concentrations. In other words, at low concentration of the dye, the ratio of active sites of adsorbent to the number of dyes molecules is high, so the adsorption becomes independent of dyes concentration.

The fast dyes adsorption on to Fe_3O_4/PMAA particles is related to the absence of internal particle diffusion resistance [39,40]. To determine the adsorption mechanism, intra particle diffusion model was introduced [41] which can be described by following equation:

$$q_t = k_d t^{1/2} \tag{2}$$

Fig. 10(b) shows the plot of the intra particle diffusion model for dyes adsorption on Fe_3O_4/PMAA particles at two concentrations (50 and 600 mg L^{-1}). As seen in

Fig. 10(b), the adsorption of MB and MR GRL on to adsorbent is affected by one step or two steps. In the porous adsorbents, three steps take place during adsorption including boundary layer diffusion, internal particle diffusion, and adsorption equilibrium. It indicates that unlike the porous adsorbents, the intra-particle diffusion is not the rate-limiting step because of high specific surface area of magnetic nanoparticles, and thus, the electrostatic interaction is the main interaction between the Fe_3O_4/PMAA adsorbent and dyes molecules.

3.2.3. Adsorption isotherms

The adsorption isotherm is the most important parameter for investigation of dye interaction with adsorbent. Fig. 11 shows the adsorption isotherms of the two cationic dyes at room temperature. The adsorption isotherms could be explained by the Langmuir and Freundlich models, expressed by the Eqs. (3) and (4), respectively. Adsorption isotherm models:

Langmuir equation:

$$\frac{C_e}{q_e} = \frac{C_e}{q_m} + \frac{1}{K_L q_m} \tag{3}$$

where q_e is the equilibrium adsorption capacity of dyes on the adsorbent (mg g^{-1}); C_e, the equilibrium ions concentration in solution (mg L^{-1}); q_m, the maximum capacity of the adsorbent (mg g^{-1}); and K_L, the Langmuir adsorption constant (L mg^{-1}).

Freundlich equation:

$$q_e = K_F C_e^{1/n} \tag{4}$$

where equilibrium capacity (q_e) and C_e are defined as above, K_F is the Freundlich constant (L mg^{-1}), and n is the heterogeneity factor. The maximum adsorption capacity (q_m) of the dyes was calculated by the Langmuir equation and is in Table 2. The considerable difference in q_m between MB and MR GRL could be

Table 2
Langmuir, Freundlich adsorption isotherm constant, correlation coefficient and q_m

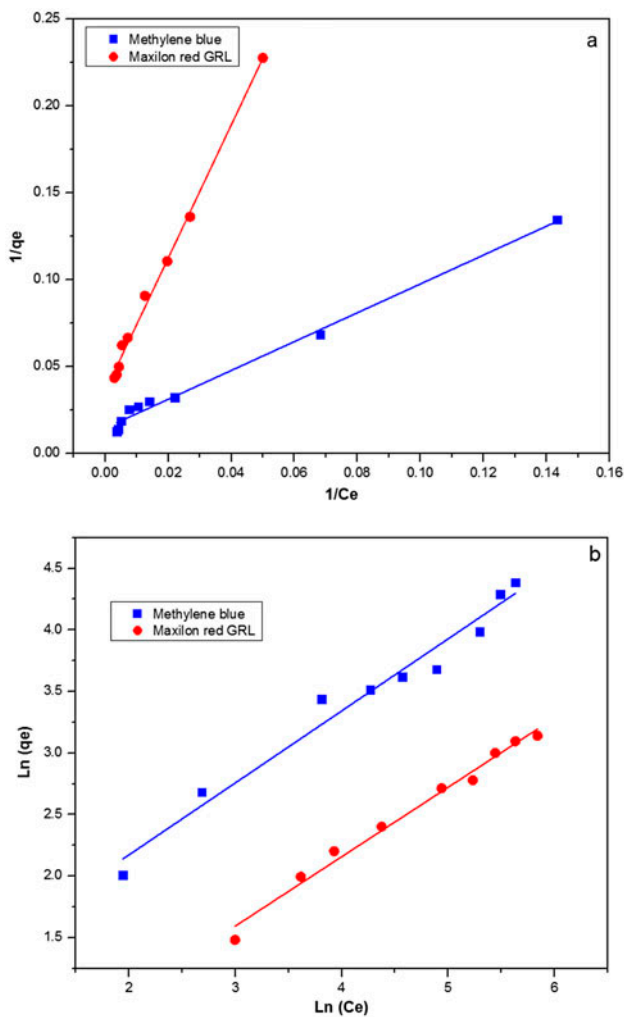| Cationic dyes	Langmuir			Freundlich		
	K_L (L mg^{-1})	q_m (mg g^{-1})	R^2	K_f ($mg^{1-1/n}$ $L^{1/n}$) g^{-1}	n	R^2
MB	0.017	68.96	0.9906	2.73	1.710	0.9661
MR GRL	0.009	27.74	0.9946	0.91	1.775	0.9846

Fig. 12. Langmuir isotherms (a) Freundlich isotherms and (b) for cationic dyes by $Fe_3O_4/PMAA$ adsorbent.

attributed to the chemical structures of the dye molecules. The fitting curves of the linear forms of the Langmuir and Freundlich models are seen in Fig. 12(a) and (b), respectively. The results showed that the equilibrium adsorption data were fitted both Freundlich and Langmuir models and slightly better described by Langmuir isotherm, indicating that the surface of adsorbent is monolayer covered with dyes molecules. According to Langmuir isotherm, the maximum adsorption capacity (q_m) of MB and MR GRL was 68.96 and 27.74 mg g^{-1}, respectively.

3.2.4. Regeneration and reuse

The reusability of adsorbents is a very important subject that should be investigated as a cost effective process in water purification. In order to regenerate
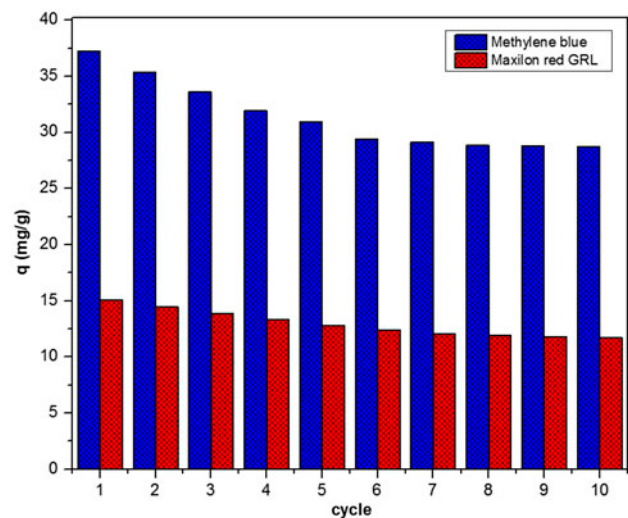

Fig. 13. Reusability of $Fe_3O_4/PMAA$ for 10 cycles, C_{dye}: 100 mg L^{-1}.

and reuse the $Fe_3O_4/PMAA$ after adsorbing dyes, the mixture solution of methanol and acetic acid was selected as the regeneration agent. Ten cycles of adsorption–desorption studies were accordingly carried out. The results are shown in Fig. 13. As seen in Fig. 13 after first cycle, the adsorption capacity of MB and MR GRL was reduced about 5 and 4%, respectively, which was due to the incomplete desorption of dyes. Also, the adsorption capacity of $Fe_3O_4/PMAA$ was retained about 78% of the fresh adsorbent after 10 cycles of desorption–adsorption. Therefore, the adsorbent shows reusability and good adsorption capacity.

4. Conclusions

In summary, $Fe_3O_4/PMAA$ nanocomposite particles were successfully prepared via one-step method and used for the removal of two cationic dyes (MB and MR GRL) from aqueous solution. The binding of PMAA onto the surface of magnetic Fe_3O_4 nanoparticles was confirmed by FTIR and TGA. The VSM results showed that $Fe_3O_4/PMAA$ has high saturation magnetization (75 µ g^{-1}) that reflects the ability of product to respond to an external magnetic field. The resulting nanocomposite particles showed pH sensitivity as determined by DLS. TEM image indicated that the product has cubic core-shell structure. The dye adsorption is mainly ascribed to the electrostatic interactions between negative charges on the $Fe_3O_4/PMAA$ surface and positive charges of dye molecules. The equilibrium data were well fitted by the Langmuir model and the adsorption capacities for MB and MR GRL in the concentration range studied were 68.96 and 27.74 mg g^{-1}, respectively. The adsorption rate

was very fast due to the absence of internal particle diffusion resistance. Moreover, the adsorbent had good reusability.

Acknowledgments

References

[1] D.T. Sponza, Toxicity studies in a chemical dye production industry in Turkey, J. Hazard. Mater. 138 (2006) 438–447.

[2] S.M.A.G. Ulson de Souza, E. Forgiarini, A.A. Ulson de Souza, Toxicity of textile dyes and their degradation by the enzyme horseradish peroxidase (HRP), J. Hazard. Mater. 147 (2007) 1073–1078.

[3] M. Muthukumar, D. Sargunamani, M. Senthilkumar, N. Selvakumar, Studies on decolouration, toxicity and the possibility for recycling of acid dye effluents using ozone treatment, Dyes Pigm. 64 (2005) 39–44.

[4] R. Malik, D.S. Ramteke, S.R. Wate, Adsorption of malachite green on groundnut shell waste based powdered activated carbon, Waste Manage. 27 (2007) 1129–1138.

[5] P. Sharma, H. Kaur, M.S.V. Sharma, A review on applicability of naturally available adsorbents for the removal of hazardous dyes from aqueous waste, Environ. Monit. Assess. 183 (2011) 151–195.

[6] M. Wawrzkiewicz, Anion exchange resins as effective sorbents for acidic dye removal from aqueous solutions and wastewaters, Solvent Extr. Ion Exch. 30 (2012) 507–523.

[7] G. Crini, Studies on adsorption of dyes on beta-cyclodextrin polymer, Bioresour. Technol. 90 (2003) 193–198.

[8] M.E. Osugi, K. Rajeshwar, E.R.A. Ferraz, D.P. de Oliveira, A.R. Araújo, M.V.B. Zanoni, Comparison of oxidation efficiency of disperse dyes by chemical and photoelectrocatalytic chlorination and removal of mutagenic activity, Electrochim. Acta 54 (2009) 2086–2093.

[9] V.K. Garg, R. Gupta, A. Bala Yadav, R. Kumar, Dye removal from aqueous solution by adsorption on treated sawdust, Bioresour. Technol. 89 (2003) 121–124.

[10] C.D. Shuang, P.H. Li, A.M. Li, Q. Zhou, M.C. Zhang, Y. Zhou, Quaternized magnetic microspheres for the efficient removal of reactive dyes, Water Res. 46 (2012) 4417–4426.

[11] L.L. Zheng, Y.L. Su, L.J. Wang, Z.Y. Jiang, Adsorption and recovery of methylene blue from aqueous solution through ultrafiltration technique, Sep. Purif. Technol. 68 (2009) 244–249.

[12] S.B. Wang, Z.H. Zhu, Effects of acidic treatment of activated carbons on dye adsorption, Dyes Pigm. 75 (2007) 306–314.

[13] A.R. Tehrani-Bagha, H. Nikkar, N.M. Mahmoodi, M. Markazi, F.M. Menger, The sorption of cationic dyes onto kaolin: Kinetic, isotherm and thermodynamic studies, Desalination 266 (2011) 274–280.

[14] A.S. Elsherbiny, M.A. Salem, A.A. Ismail, Influence of the alkyl chain length of cyanine dyes on their adsorption by Na^+-montmorillonite from aqueous solutions, Chem. Eng. J. 200–202 (2012) 283–290.

[15] L. Liu, Y. Wan, Y. Xie, R. Zhai, B. Zhang, J. Liu, The removal of dye from aqueous solution using alginate-halloysite nanotube beads, Chem. Eng. J. 187 (2012) 210–216.

[16] Y. Yu, Y.Y. Zhuang, Z.H. Wang, M.Q. Qiu, Adsorption of water-soluble dyes onto resin NKZ, Ind. Eng. Chem. Res. 42(26) (2003) 6898–6903.

[17] L.H. Reddy, J.L. Arias, J. Nicolas, P. Couvreur, Magnetic nanoparticles: Design and characterization, toxicity and biocompatibility, pharmaceutical and biomedical applications, Chem. Rev. 112 (2012) 5818–5878.

[18] I. Ali, New generation adsorbents for water treatment, Chem. Rev. 112 (2012) 5073–5091.

[19] S. Sun, H. Zeng, Size-controlled synthesis of magnetite nanoparticles, J. Am. Chem. Soc. 124 (2002) 8204–8205.

[20] D.K. Kim, M. Mikhaylova, Y. Zhang, M. Muhammed, Protective coating of superparamagnetic iron oxide nanoparticles, Chem. Mater. 15 (2003) 1617–1627.

[21] A. Ditsch, P.E. Laibinis, D.I.C. Wang, T.A. Hatton, Controlled clustering and enhanced stability of polymer-coated magnetic nanoparticles, Langmuir 21 (2005) 6006–6018.

[22] S.H. Huang, M.H. Liao, D.H. Chen, Fast and efficient recovery of lipase by polyacrylic acid-coated magnetic nano-adsorbent with high activity retention, Sep. Purif. Technol. 51 (2006) 113–117.

[23] M.T. Pham, K.K. Soo, Surface functionalized nano-magnetic particles for wastewater treatment: Adsorption and desorption of mercury, J. Nanosci. Nanotechnol. 9 (2009) 905–908.

[24] H.Y. Zhu, R. Jiang, L. Xiao, Adsorption of an anionic azo dye by chitosan/kaolin/γ-Fe_2O_3 composites, Appl. Clay Sci. 48 (2010) 522–526.

[25] Y.R. Zhang, S.Q. Wang, S.L. Shen, B.X. Zhao, A novel water treatment magnetic nanomaterial for removal of anionic and cationic dyes under severe condition, Chem. Eng. J. 233 (2013) 258–264.

[26] Y.P. Chang, C.L. Ren, Q. Yang, Z.Y. Zhang, L.J. Dong, X.G. Chen, D.S. Xue, Preparation and characterization of hexadecyl functionalized magnetic silica nanoparticles and its application in Rhodamine 6G removal, Appl. Surf. Sci. 257 (2011) 8610–8616.

[27] D.P. Li, Y.R. Zhang, X.X. Zhao, B.X. Zhao, Magnetic nanoparticles coated by aminoguanidine for selective adsorption of acid dyes from aqueous solution, Chem. Eng. J. 232 (2013) 425–433.

[28] B. Zargar, H. Parham, A. Hatamie, Fast removal and recovery of amaranth by modified iron oxide magnetic nanoparticles, Chemosphere 76(4) (2009) 554–557.

[29] Z. Zhang, J. Kong, Novel magnetic Fe_3O_4@C nanoparticles as adsorbents for removal of organic dyes from aqueous solution, J. Hazard. Mater. 193 (2011) 325–329.

[30] L.M. Zhou, J.Y. Jin, Z.R. Liu, X.Z. Liang, C. Shang, Adsorption of acid dyes from aqueous solutions by the ethylenediamine-modified magnetic chitosan nanoparticles, J. Hazard. Mater. 185 (2011) 1045–1052.

[31] A. Debrassi, A.F. Corrêa, T. Baccarin, N. Nedelko, A.S. Lawska-Waniewska, K. Sobczak, P. Dłu_zewski, J.M. Greneche, C.A. Rodrigues, Removal of cationic dyes from aqueous solutions using N-benzyl-O-carboxymethylchitosan magnetic nanoparticles, Chem. Eng. J. 183 (2012) 284–293.

[32] L.L. Fan, Y. Zhang, C.N. Luo, F.G. Lu, H.M. Qiu, M. Sun, Synthesis and characterization of magnetic β-cyclodextrin–chitosan nanoparticles as nano-adsorbents for removal of methyl blue, Int. J. Biol. Macromol. 50 (2012) 444–450.

[33] H.Y. Zhu, Y.Q. Fu, R. Jiang, J. Yao, L. Xiao, G.M. Zeng, Novel magnetic chitosan/poly(vinyl alcohol) hydrogel beads: Preparation, characterization and application for adsorption of dye from aqueous solution, Bioresour. Technol. 105 (2012) 24–30.

[34] L. Adamčíková, K. Pavlíková, P. Ševčík, The decay of methylene blue in alkaline solution, React. Kinet. Catal. Lett. 69 (2000) 91–94.

[35] S. Wang, Y. Zhou, W. Sun, Preparation and characterization of antifouling thermosensitive magnetic nanoparticles for applications in biomedicine, Mater. Sci. Eng. C 29 (2009) 1196–1200.

[36] S. Khoee, H. Shagholani, N. Abedini, Synthesis of quasi-spherical and square shaped oligoamino-ester graft-from magnetite nanoparticles: Effect of morphology and chemical structure on protein interactions, Polymer 56 (2015) 207–217.

[37] Y.Y. Xu, M. Zhou, H.J. Geng, J.J. Hao, Q.Q. Ou, S.D. Qi, H.L. Chen, X.G. Chen, A simplified method for synthesis of Fe_3O_4@PAA nanoparticles and its application for the removal of basic dyes, Appl. Surf. Sci. 258 (2012) 3897–3902.

[38] D. Wang, L. Liu, X. Jiang, J. Yu, X. Chen, Adsorption and removal of malachite green from aqueous solution using magnetic β-cyclodextrin-graphene oxide nanocomposites as adsorbents, Colloids Surf., A: Physicochem. Eng. Aspects 466 (2015) 166–173.

[39] Y.B. Song, S.N. Lv, C.J. Cheng, G.L. Ni, X.W. Xie, W. Huang, Z.G.Z. Hao, Fast and highly-efficient removal of methylene blue from aqueoussolution by poly (styrenesulfonic acid-co-maleicacid)-sodium-modified magnetic colloidal nanocrystal clusters, Appl. Surf. Sci. 324 (2015) 854–863.

[40] Y.C. Chang, D.H. Chen, Preparation and adsorption properties of monodisperse chitosan-bound Fe_3O_4 magnetic nanoparticles for removal of Cu(II) ions, J. Colloid Interface Sci. 283 (2005) 446–451.

[41] R. Shukla, G. Madras, Facile synthesis of aluminium cobalt oxide for dye adsorption, J. Environ. Chem. Eng. 2 (2014) 2259–2268.